Encapsulation of Fillers with Grafted Polymers for Model Composites

I. LUZINOV,[1] A. VORONOV,[1] S. MINKO,[1,*] R. KRAUS,[2] W. WILKE,[2] and A. ZHUK[3]

[1]Lviv Department of Physical Chemistry Institute, Naukova 3a, Lviv, 290053, Ukraine, [2]Abteilung Experimentelle Physik, Universität Ulm, D-89069 Ulm, Germany, and [3]Division of Applied Science, Harvard University, Cambridge, Massachusetts

SYNOPSIS

Glass beads were encapsulated by grafted polymers: polybutylacrylate and polystyrene. Grafting was performed by the polymerization initiated from the particle surface with preliminary adsorbed polyperoxide initiator. Grafting procedure and properties of grafted film were studied using model substrates: powders, plates, and wafers by wetting technique and SEM. Conditions of grafting affect the film structure. They are porous, and due to some sort of pores the wetting liquid is able to penetrate into covering and reach the substrate. Model epoxy composites were prepared with covered glass beads. The coverings allowed a decrease of adhesion between the matrix and bead surface to detect acoustic emission caused by the debonding process. The dependence of debonding stress from covering the structure and nature was studied. © 1996 John Wiley & Sons, Inc.

INTRODUCTION

The effect of interphase and interface interaction on mechanical behavior, including the mechanism of microdefects nucleation and propagation, for polymer composites has been of great interest in recent time.[1-3] Questions of the investigation of an interphase structure inside composites are the reason that studying of a beforehand tailored and controlled interphase seems to be more preferential.[4] Obviously, this way also has a pragmatic application.

Polymer covering on the solid surface usually is obtained due to a plain physisorption of a polymer from the solution,[5] by grafting from solid surface (e.g., refs. 6–11), or by film formation of a polymer or prepolymer from the solution due to the evaporation of the solvent and subsequent polymerization or some other treatment.[12] Polymer covering could effect weak adhesion and fracture of composites even if the covering is obtained from the same polymer as the matrix.[6] In other cases it improves adhesion,[8,11] impact, and fracture properties,[11,12] or influences the nucleation of cracks or crazes.[7]

The effect of the interphase on mechanical behavior of the composite is caused by two reasons. The first is the adhesion between interphase, filler, and matrix.[1-3] On the other hand, the interphase effects the stress field around the inclusion[13,14] due to its elastic properties (very different from matrix) and definite thickness. Both reasons affect the area and conditions of crack nucleation and propagation. Obviously, the effect of interlayer on filler–matrix adhesion is influenced by its composition and structure. Interlayer structure in most cases means a conformation of polymer chains determined by molecular weight, surface concentration, and interaction with the substrate and matrix. There are a lot of theoretical works that predict a structure of adsorbed or grafted chains (e.g., refs. 5,15,16), but there are few experimental studies about the detailed investigation of grafted polymer film structure.[17-19] Details of the interphase structure usually are rarely considered in most works devoted to the effect of the interphase on mechanical behavior of composites.

On the other hand, information about the structure of polymer coverings is necessary to compare with the detailed information about fracture mechanism on a not only a macroscopic but

* To whom correspondence should be addressed.

Journal of Applied Polymer Science, Vol. 61, 1101–1109 (1996)
 CCC 0021-8995/96/071101-09

also a microscopic level. Among various tests of composites the nondestructive methods seem to be very promising for fracture mechanism investigation, especially acoustic emission and small-angle scattering.[20,21]

We are especially interested in the problem of a combination of synthesis of polymer covering on the filler and fiber surface and a detailed study of its structure and the mechanical behavior of composites.

The aim of this article is to describe the synthesis of polymer coverings of various composition and structure on the surface of glass beads that were used as fillers for model epoxy composites. Debonding processes under tensile stress were investigated by the acoustic emission technique. As a model filler we also used various powders of inorganic oxides with the specific surface (s) higher than the one for glass beads to improve the accuracy of measurements of the grafting process. The copolymer of peroxide monomer (PM) 5-tertbutyl-peroxy-5-methyl-1-hexen-3-yne and maleic anhydride (MA) was used as a polymer initiator (PI) of grafting from the filler surface. Ordinary physisorption of PI is a very suitable technique to immobilize peroxide groups on any polar solid surface.[22]

EXPERIMENTAL

Materials

Styrene (St), butylmethacrylate (BMA), butylacrylate (BA), ethylacrylate (EA), nonylacrylate (NA), and methylmethacrylate (MMA) of reactive grade were distilled under reduced pressure with argon.

PI[23] (47 : 53 mol of PM : MA) M_n = 2800, M_w = 3200, and dicumene peroxide (DCP) were obtained from the Organic Chemistry Department of Lvivska Politechnica State University and used without further purification.

Butylacetate of reactive grade was used as received.

Glass beads (Pyrex) were obtained from the MO-SCI Corporation. Six fractions of beads with diameters 50–63, 80–90, 90–106, 100–125, 160–200, and 315–400 μm were used as received. Powders of aluminum oxide (s = 0.05 m^2/g) of reactive grade, TiO_2 (industry pigment s = 1.0 m^2/g), ZnO (industry pigment s = 0.6 m^2/g) were rinsed in butylacetate and dried at 120°C.

Aluminum, titanium, and zinc foil, plates of Pyrex glass, and silicon wafers were rinsed with butylacetate and heated at 500°C. We anticipated that the surface of the metal foil is covered with thin oxide film and could be considered as the model of corresponding oxide surface.

Grafting

Peroxide groups were attached to the solid surface due to PI adsorption from 0.5% solution in butylacetate for ratio adsorbent : solution = 1 : 4 by weight (for powders), that corresponds to the saturated adsorbed layer of PI.[22] The adsorption amount was evaluated by pyrolysis at 500°C. For glass beads, we performed a special experiment using milled glass beads to increase the specific surface (up to 0.05 m^2/g) and the accuracy of the measurement. The amount of adsorbed PI for all powders was about 9 $\pm$ 1 mg/m^2. Powders were separated by centrifugation, rinsed with butylacetate to remove unadsorbed PI (adsorbed PI will not be removed in this conditions),[22] and dried at an ambient temperature. The same procedure was used to modify plates and wafers.

Modified powders, monomer, additional initiator DCP (see below), and solvent were placed into the reaction vessel under nitrogen and constant stirring and heated in a oil bath at a given polymerization temperature with a various duration. The encapsulation of glass beads was made in a rotary reaction vessel (to avoid an damage of the beads). Grafting from plates was performed under shaking of the reaction tube.

The separation of the powders from the medium was carried out by centrifugation. Powders, beads, and plates were rinsed six times in butylacetate to wash away ungrafted polymer and dried *in vacuo* at 60°C. For a special experiment only one washing procedure was made (see below).

The grafting amount was evaluated by pyrolysis at 500°C; relative error was not more than 10% for powders and 20% for glass beads.

Usually, the grafting procedure was performed simultaneously for powders (beads) and plates (wafers). The first ones were used for evaluation of the grafted amount or preparation of model composites, and the second one for the contact angle measurements and SEM.

Contact Angle Measurements

A drop (0.001 mL) of double distilled water with a microliter syringe or epoxy resin (diglycidil-ether of bisphenol A-DGEBA) was put on the plate with a glass tip. We used DGEBA as a model because the epoxy resin used for composites was in a solid state

at room temperature. Diameter (d) and height (h) of the drop was measured by a cathetometer at room temperature. The contact angle value was computed as $\tan(\Theta/2) = 2h/d$ ($\pm 1°$). Contact angles for the substrate covered by the grafted polymer (Θ_{gr}) or by PI were compared with the ones for "pure" plates and a thick polymer film of the given polymer (Θ_p) obtained from a concentrated solution.

Preparation of Composites

The specimens were prepared by the mixing of the epoxy resin (resorcinol diglycidil ether and *m*-phenylenediamine under stochiometric ratio), the initiator, and the filler and polymerized under rotation at $T = 64°C$ to avoid precipitation of the filler particles and with further curing by a two-step temperature procedure ($T = 64°C$, 4 h, $T = 130°C$, 8 h). The filler consists of glass beads of various size (50–63, 80–90, 100–125, 160–200, 315–400 μm) with a volume fraction of 1% for all sizes.

Scanning Electron Microscopy

The pictures of the fracture surface of composites and wafers with grafted polymer layers were obtained with a JEOL JSM-1300 instrument at 35 kV and with a ZEISS DSM 962 instrument at 10–20 kV.

Test Methods

Tensile tests were performed on a Zwick 1445 testing machine at a constant speed of $d\lambda/dt = 1.25 \cdot 10^{-3}$ s^{-1} ($\lambda = L/L_0$). Acoustic emission was monitored on an AET Model 5500 system. The AET 5500 was set up in single sensor mode with one transducer attached to the specimen by a spring clamp. The transducer was a standard AET AC175L with a resonant frequency of 175 kHz and a sensitivity better than -72 dB referred to 1 V/μbar. The detected signals were passed through a bandpass filter FL-12 with a flat frequency response between 125 and 250 kHz. Then they were preamplified in an AET Model 140/160B preamplifier with a total gain of 40/60 dB and a flat frequency response between 1 kHz and 2 MHz. Final amplification was performed by the AET Signal Processing Unit with 30 dB. To eliminate noise events only acoustic emission events with three or more ring down counts (number of threshold crossings by the signal voltage) were accepted.[24]

The type of preamplifier and the event duration clock settings were adjusted to match the dynamic range of the acoustic emission system to the individual conditions in terms of signal amplitude and event duration. For a resonant transducer, the event duration is related ($\approx$ prop.) to the signal amplitude.[25] Therefore, low peak amplitude signals require a high preamplifier gain and short clock counter intervals for maximum signal resolution, while high peak amplitude signals need a low preamplifier gain and longer clock counter intervals to avoid amplifier overload and duration counter overflow.

The force and deformation data were input into the AET 5500 through the analog input channels. As the most part of the specimen is covered with clamp and sensor, optical strain measurement cannot be used here. The deformation of the samples is practically homogeneous. Therefore, the strain λ is determined from the traverse distance ΔL by $\lambda = (\Delta L + L_0)/L_0$. For each acoustic emission event strain (λ), stress (σ), peak amplitude ($A = 20 \cdot \log_{10}(U/U_{ref})$ [dB], U: signal voltage, U_{ref}: reference voltage), event duration, and number of ring down counts (i.e., threshold crossings) are recorded.[21]

RESULTS AND DISCUSSION

Investigation of Grafting

The scheme of the synthesis of the polymer covering on the solid surface is shown in Figure 1. The peroxide initiator is attached to the solid surface as the first step. Adsorbed PI due to MA units is strongly adhered to the oxide or glass surface, forming hydrogen bonds with surface hydroxyls. We may anticipate that gradually due to water traces in the solvent and adsorbed water MA units hydrolyze. It is not very important whether anhydride or carboxyl groups form hydrogen bonds on the surface. The most important fact is that PI is strongly adhered due to the physical adsorption, and any ingredients will not displace PI from the surface.[22]

Contact angles of wetting of the unmodified and modified plates by water and DGEBA are presented in Table I. Contact angles for substrate covered by PI are lower as the ones for thick film of PI. Consequently, PI even in saturated adsorbed layer does not insulate the substrate surface. Adsorbed skin is permeable for the wetting liquid and may be considered as a porous one.[26]

On the next step at heating due to the thermolysis of peroxide groups of adsorbed PI, two sorts of free radicals form: macroradicals adhered to the solid surface and *tert*-butoxy radicals diffusing into the bulk. Both radicals initiate the polymerization and produce two sorts of polymer: grafted copolymer ad-

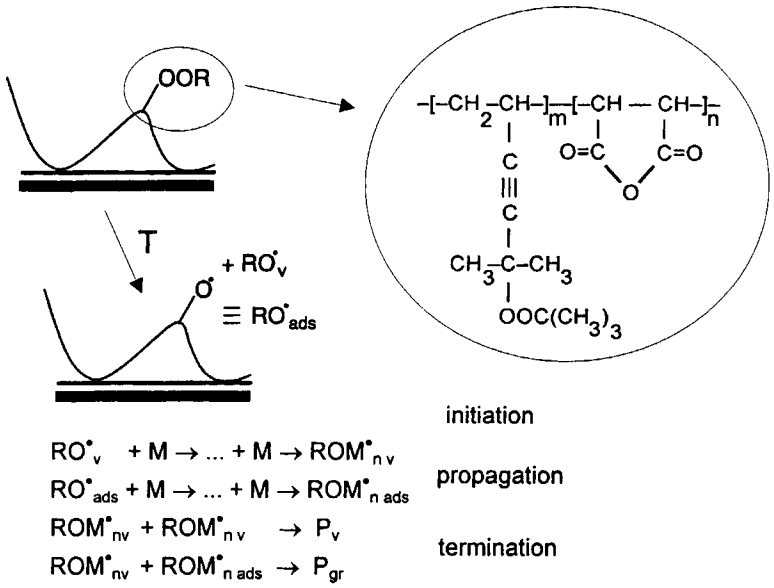

Figure 1 Grafting polymerization on the solid surface covered by PI: $RO^{\bullet}_{ads}$ and $RO^{\bullet}_{v}$–macroradical adsorbed on the substrate and *tert*-butoxy radical diffusing to the bulk, respectivly.

hered to the solid surface and homopolymer in the bulk. Thus, we did not graft a monomer to the substrate, but actually we grafted a monomer to the PI, which was absorbed on the surface. Besides, the additional initiator, DCP, was added to the monomer solution. In fact, the specific surface of most powders was low and the amount of the initiator in the reaction mixture was too small. Even small traces of an inhibitor or oxygen could hamper the progress of grafting. Additional initiator was added as much (0.1–1% by weight of solution) that the rate of the polymerization in the bulk was influenced mainly by DCP. Termination of free radicals attached to the solid surface occurs mainly in the reaction with radicals from the bulk.[27] Consequently, we can control the molecular weight of the grafted chains using definite concentration of an additional initiator. Following the separation and rinsing procedure, we obtain filler particles covered with the grafted copolymer. The anchoring part of the copolymer interacts with the substrate surface due to hydrogen bonds. Side chains of polystyrene or polyacrylates are grafted to the anchor chain. Characteristics of the coverings obtained under similar conditions are shown in the Table II. The amount of grafted polymer does not depend on substrate nature and the grafting monomer. The common behavior of all specimens is that they do not completely insulate the substrate surface ($\Theta_{gr} < \Theta_P$). The coverings are porous.

We performed an experiment in which after the grafting the encapsulated substances were split into two parts. One part was rinsed as usually six times, and for the second, we performed only one washing procedure. In the last case, ungrafted chains being entangled with grafted polymer were not washed away. Ungrafted chains formed by unattached free radicals during the polymerization have not sufficient time to diffuse to the bulk because of poor diffusivity of the polymer. They are kept, due to en-

Table I Contact Angles (DEG) for Wetting of Substrates Uncovered and Covered by PI

	Water		Epoxy Resin DGEBA	
Substrate	Uncovered	Covered by PI	Uncovered	Covered by PI
Al_2O_3	38	53	—	—
Pyrex	7	22	36	55
Thick film of PI	—	77	—	69

Table II Grafting on Substrates Modified by PI (T = 95°C, 6 h, [M] = 20%, [DCP] = 0.5% by Weight of Solution)

Grafted Polymer	Substrate	Grafting Amount/mg/m^2	Θ_p/DEG	Θ_{gr}/DEG
PBA	Al_2O_3	17.4	91	56
PEA	Al_2O_3	18.0	88	63
PNA	Al_2O_3	19.2	99	72
PMMA	Al_2O_3	16.2	76	69
PBMA	Al_2O_3	18.4	82	58
PSt	Al_2O_3	15	90	80
PMMA	TiO_2	16.3	76	71
PMMA	ZnO	10.5	76	65
PMMA	Pyrex	16.1	76	63

tanglement with the grafted layer. The dependence of the grafted amount on the time of polymerization on the powder of Al_2O_3 is shown in Figure 2 for two sorts of washing procedures. The corresponding relationships for contact angles are given in Figure 3. During polymerization the fraction of the ungrafted polymer increases and reaches 50% of the total amount of the polymer in the covering. The plot of the relationship Θ_{gr} vs. the amount of the polymer in covering shows a plateau in both cases. The plateau is reached very soon after the beginning of the polymerization.

The covering that was washed one time insulates the surface completely. The film washed six times incompletely insulates the substrate even in the plateau area. Consequently, the covering consisting of the grafted and ungrafted polymer is obtained. After multiple washings the ungrafted polymer was washed away and pores were created. The porosity of the covering depends on the grafting amount. Above a definite value of grafting, porosity becomes independent from the grafting value. This interesting behavior can be explained by two reasons. Because of poor efficiency of the initiation reaction, the most fraction of the peroxide groups of PI does not initiate the polymerization. In the area of ineffective decomposition, gaps are formed. These gaps are filled with ungrafted polymer, which then will be washed away. Secondly, ungrafted polymer blocks some areas on the substrate surface and gaps are formed because of steric control of the grafting.

From the relationship between Θ_{gr} and the time of BMA grafting (Fig. 4) it is clear that the higher monomer concentration results in lower porosity of the covering. We anticipate that increasing the monomer concentration effects higher efficiency of the initiation of the graft polymerization. This fact proves the first above-mentioned reason of the porosity. Polymerization in harder conditions (T = 110°C, [M] = 4.5 mol/l) leads to completely insulated substrate already in the beginning of the process (Table III).

Plots of the grafted amount of PBA and PSt vs. total monomer conversion are shown in Figure 5. A

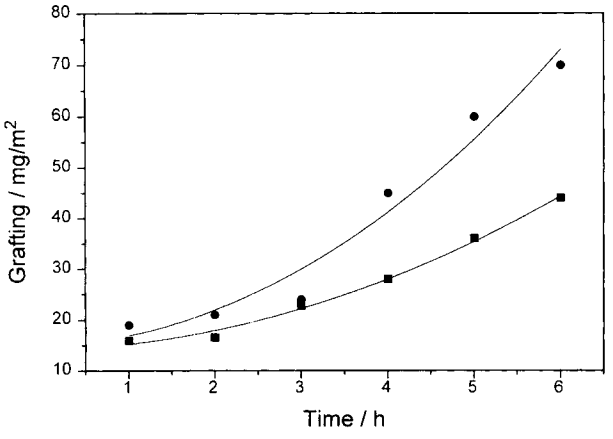

Figure 2 Polymer in the covering vs. time of polymerization (●—one washing, ■—six washing procedures).

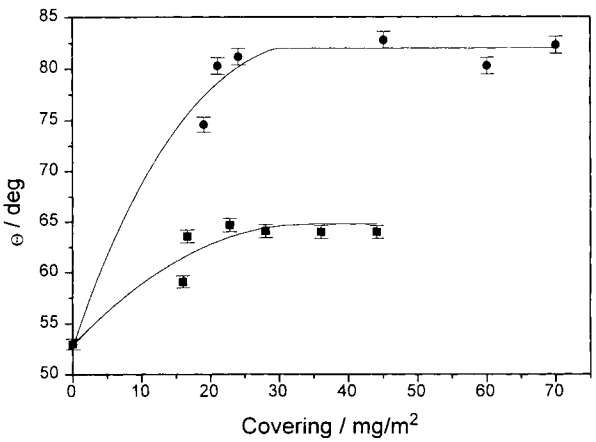

Figure 3 Contact angle for wetting of grafted covering by water (●—one washing, ■—six washing procedures).

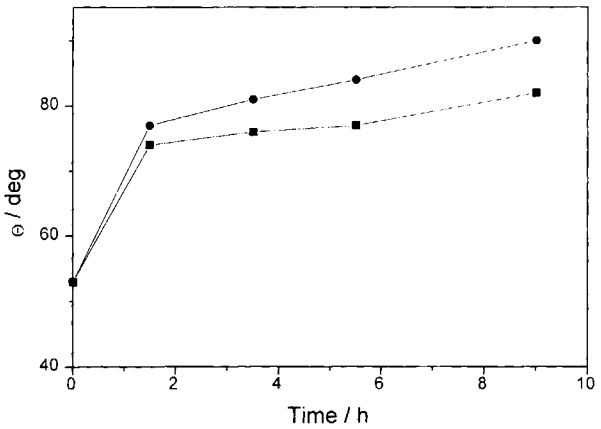

Figure 4 Contact angle vs. time of PBMA grafting (●—[M] = 3 mol/l, ■—[M] = 1 mol/l).

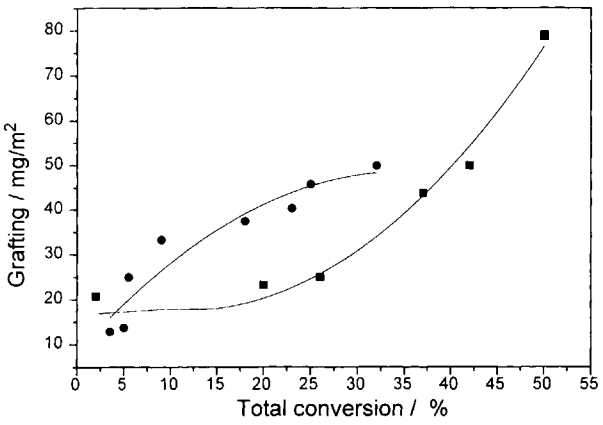

Figure 5 Grafting of St (●) and BA (■) at T = 110°C, [M] = 4.5 mol/l.

great difference between the two curves was obtained. It was observed in the hard conditions of polymerization and after grafting an amount of about 20 mg/m^2. Polystyrene polymerization is followed by a decrease of rate, while BA polymerization runs with acceleration. The contact angle for both cases reaches its maximum (Table III) practically immediately, and the substrate is completely insulated with the grafted polymer. This rises the question, what was the mechanism that increases the grafted amount. Obviously, increasing of the surface concentration of the grafted chains is followed by a change of their conformation. Chains extend in the direction normal to the substrate surface that causes them to vacate the area. This process runs within a definite limit, and following grafting, it becomes hardly probable. This model seems to be valid for styrene grafting. In the case of BA, we suppose that at the surface film the situation was similar to the Trommsdorf effect for polymerization in the bulk. The rate of the termination reaction decreases due to chain interactions. The latter causes an increase of the rate of polymerization and molecular weight of polymer. On the other hand, for Trommsdorf effect conditions the probability of chain transfer reaction to the polymer is higher. Both facts cause the formation of a polymacromolecule (multilayer) covering with crosslinking of chains. Thus, due to the Trommsdorf effect conditions, an unlimited thick covering could be obtained.[27] Despite the fact that

Table III Grafting on Glass Beads Modified by PI (T = 110°C, [M] = 4 mol/L, [DCP] = 0.1% by Weight of Solution)

Grafted Polymer	Time of Grafting/h	Grafting Amount/mg/m^2	Calculated Thickness/nm	Contact Angle/DEG	
				Water	DGEBA
Polystyrene	0.5	12.9	12	89	68
	1	13.8	13	90	69
	2	25	24	90	70
	4	33.3	31	90	71
	6	37.5	35	90	71
	8	40.4	38	90	71
	11	45.8	43	90	71
	15	50	47	90	71
Polybutylacrylate	0.5	20.8	20	90	61
	1	23.3	23	91	62
	1.5	25	24	91	62
	2	43.8	43	91	62
	2.5	50	49	91	62
	8	79.1	77	91	62

the Trommsdorf effect is known for both St and BA polymerization, a thick covering was obtained only for BA, obviously because of a considerably higher pronounced Trommsdorf effect for BA and substantial differences of propagation and chain transfer reaction constants for these monomers. Crosslinking of chains was prooved in a model experiment. The grafting of PBA was performed on $CaCO_3$ particles with adsorbed PI on the surface. Then we dissolve the covered $CaCO_3$ in dilute HCl. Polymer films were separated. It turned out that they were insoluble in any solvent.

Encapsulation of Glass Beads

In this work we performed covering of the glass beads for a model composite in conditions that cause continuous covering impermeable for the wetting liquid, due to the above-mentioned results, which could be achieved at a high surface density of grafted chains. The latter we reached due to hard conditions (T = 110°C, [M] = 4.5 mol/l). Characteristics of the obtained specimens of the fraction 90–106 μm are presented in Table III. The thickness was calculated due to an assumption that the density of polymer in the film is the same as in the bulk. Calculated values are lower than ones visible in the SEM pictures for model specimens with the covering on silica wafers (Fig. 6). This is the proof of a more complicated structure of the covering. Obviously, the above-mentioned presumption about layer density is not valid, and thick covering is also "porous." These pores are not permeable for wetting liquid to get the substrate surface.

Thus, we prepared glass beads covered by uniform films of PBA and PSt of various thicknesses. The latter was obtained due to a change of chain conformation following an increase of the grafting density and also by formation of multilayers in chain transfer reaction to the polymer.

Mechanical Behavior of Composites

Excellent adhesion between epoxy matrix and uncovered glass beads causes the debonding to occurr only at the stress of the fracture. Crack nucleation proceedes in the matrix and leads to a specimen break prior to completion of the debonding process. Therefore, the debonding processes could not be investigated by the acoustic emission technique.

A plot of the acoustic emission rate ($dN/d\sigma$) vs. stress typically for most specimens filled by covered beads is shown in Figure 7. $dN/d\sigma$ was calculated as the number of acoustic emission events that occur

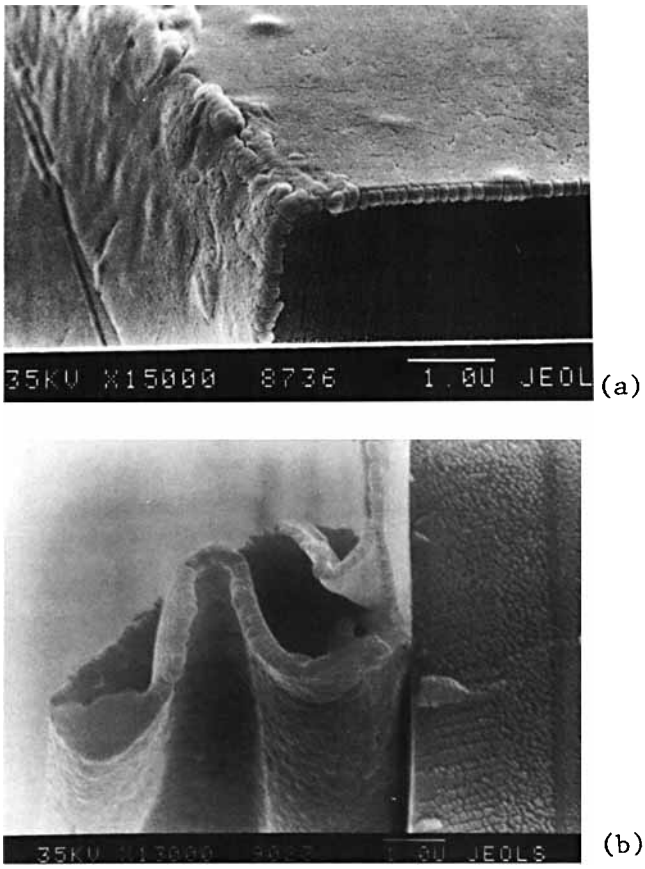

Figure 6 SEM pictures of the fracture surface of silicon wafer covered by grafted PSt (a), the same covering pilled off from Cu substrate with dilute acid (b).

in a stress interval of $\Delta\sigma$ = 1 MPa. The plot shows two maxima. Investigation of the debonding by optical microscopy showed that each maximum of the acoustic emission rate corresponds to debonding on one side of the beads. The spherical particles debond on the polar sides. The first stage of debonding decreases the local stress concentrations on the filler surface. With a further increase of applied stress, the local stress grows again until the second side of the filler particle is debonded, too.

The average amplitude <A>(σ) was calculated as the mean value of the peak amplitude of all AE events within a stress interval $\Delta\sigma$ = 1 MPa. It rises with increasing stress, reaches its maximum at the stress of debonding σ_d, and decreases with a further increase of the stress (Fig. 7). At the second stage, the average amplitude has a second maximum but with a lower peak amplitude. This correlation between the acoustic emission rate and the average acoustic emission rate is typical for all coverings and filler sizes.

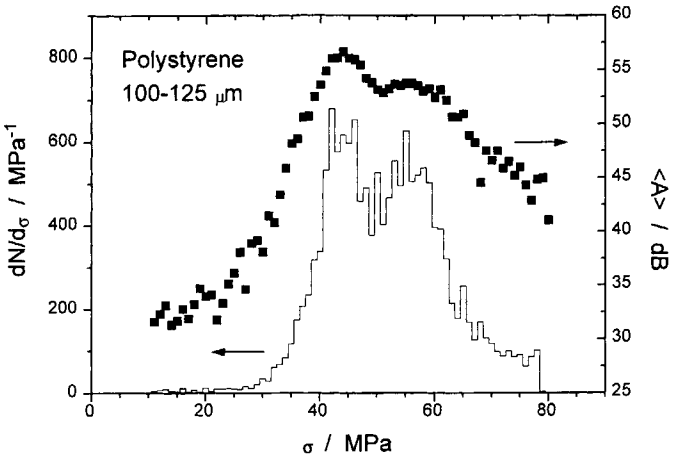

Figure 7 Behavior of acoustic emission rate and mean peak amplitude during loading. Model composite with glass beads (100–125 μm) coated with polystyrene.

Values of debonding stress for different fractions of beads with PSt and PBA coverings are shown in Table IV. Debonding stress increases in the range for coverings: Pst < PBA < adsorbed PI < uncovered surface. Obtained results are interesting to compare with SEM pictures of fracture surface (Fig. 8). For the case of lowest adhesion [PSt covering, Fig. 8(a)], the matrix is completely debonded from covering. For beads with PBA covering [Fig. 8(b)], areas of debonding are covered with "stars" of similar shape that are distributed uniformly on the bead surface. We suppose that due to the matrix–covering interaction, interpenetration of both polymers takes place especially because of the porous properties of the covering. But this interaction is not very strong and debonding occurs at the covering–matrix interface. For covering of adsorbed PI [Fig. 8(c)], the debonding surface looks like a fraction of the matrix remained on the filler surface. Because PI does not completely insulate the glass surface, the debonding occurs by matrix fracture in the points, where matrix penetrated through the PI layer and reached the glass surface. In the areas of contact between matrix and PI chains the debonding occurs between the covering and the matrix. That causes an irregular shape of the surface of debonding.

Table IV Debonding Stress Data

Covering	Bead Size/μm	Debonding Stress/MPa
PI	50–63	81
	100–125	83
	160–200	77
PSt	50–63	43
	100–125	43
	160–200	42
	315–400	33
PBA	50–63	61
	80–90	72
	160–200	75

CONCLUSIONS

Due to the grafting polymerization from the polymer initiator adsorbed on the solid surface, the polymer coverings of various thickness and porosity were obtained.

The grafted amount of polystyrene reaches a plateau during grafting. Due to the Trommsdorf effect for the polymerization at the interphase, grafting of PBA grows without limit.

At least two sorts of porosity could be controlled. Due to the first one, wetting liquid (or matrix prepolymer) could interpenetrate through the covering and contacts with the substrate. Due to the second one, density of the covering is lower than the density of the polymer in the bulk, and interpenetration of both the polymer of the covering and the matrix is possible.

Glass beads covered by PSt and PBA have lower adhesion to epoxy matrix than uncoverd ones. That allowed detection of the debonding process in model composites before the stress of fracture. Relationship between acoustic emission rate and stress showed two maxima. Each maximum of the acoustic emission rate corresponds to debonding on one side of the beads. The value of the debonding stress depends on the covering structure.

We propose in our next article to discuss in details of the results of acoustic emission tests.

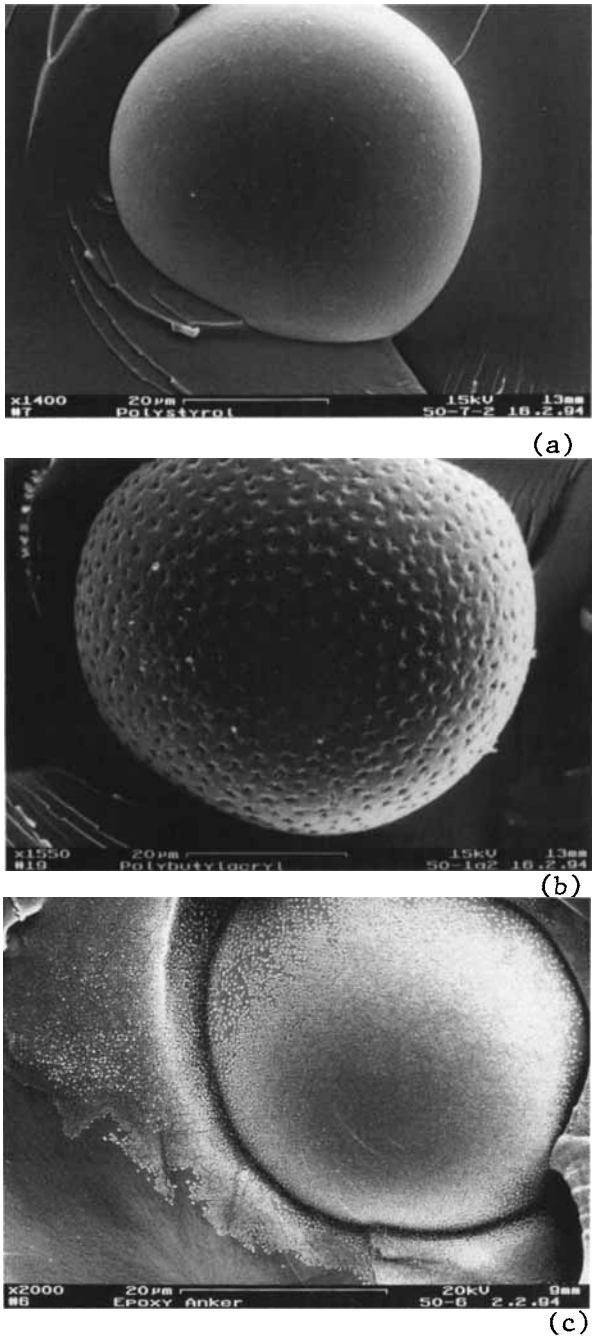

Figure 8 SEM pictures of the fracture surface of model epoxy composites filled with covered glass beads by: (a) PSt, (b) PBA, (c) PI.

We are grateful for the support of NATO Scientific and Environmental Affairs Division by providing an Linkage Grant under HTECH..LG 940579 to improve cooperation. Initial collaboration and acoustic emission experiments were supported by the Sonderforschungsbereich 239 of the Deutsche Forschungsgemeinschaft (DFG). The authors are very much indebted to the Organic Chemistry Department of Lvivska Polytechnika State University for the samples of peroxide initiators and PI.

REFERENCES

1. D. Hull, *An Introduction to Composite Materials,* Cambridge University Press, Cambridge, 1981.
2. H. Ishida and G. Kumar, in *Molecular characterization of Composite Interfaces,* Plenum Press, New York, 1983.
3. R. J. Young, in *Structural Adhesives,* A. J. Kinloch, Ed., Elsevier, New York, 1986, p. 186.
4. A. Pavan, *Chimia,* **44,** 360 (1990).
5. M. Kawaguchi, *Prog. Polym. Sci.,* **18,** 341 (1993).
6. G. C. Eastmond and G. Mucciariello, *Polymer,* **23,** 164 (1982).
7. G. F. Abate and D. Heikens, *Polym. Commun.,* **24,** 342 (1983)
8. S. Shkolnik and H. Hocker, *Polymer,* **33,** 1669 (1992).
9. J. Liang, J. P. Bell, and D. A. Scola, *J. Appl. Polym. Sci.,* **48,** 477 (1993).
10. N. Tsubokawa and H. Ishida, *J. Polym. Sci, Part A: Polym. Chem.,* **30,** 2241 (1992).
11. G. Boven, R. Folkersma, G. Challa, A. J. Schouten, and M. Bosma, *Polymer,* **33,** 83 (1992).
12. N. Amdouni, H. Sautereau, J. F. Gerard, F. Fernagut, G. Coulon, and J. M. Lefebvre, *J. Mater. Sci.,* **25,** 1435 (1990)
13. L. J. Broutman and B. D. Agarwal, *Polym. Eng. Sci.,* **14,** 581 (1974).
14. T. Ricco, A. Pavan, F. Danusso, *ibid,* **14,** 774 (1978).
15. P-Y. Lai and K. Binder, *J. Chem. Phys.,* **97,** 586 (1992)
16. C. Young, A. C. Balazs, and D. Jasnow, *Macromolecules,* **26,** 1914 (1993).
17. S. J. O'Shea, M. E. Welland, and T. Rayment, *Langmuir,* **9,** 1826 (1993).
18. W. Zhao, G. Kraush, M. H. Rafailovich, and J. Sokolov, *Macromolecules,* **27,** 2933 (1994).
19. D. F. Siquiera, K. Köhler, and M. Stamm, *Langmuir,* **11,** 3092 (1995).
20. J. Bohse and G. Kroh, *J. Mater. Sci.,* **27,** 298 (1992).
21. R. Kraus, A. Payer, and W. Wilke, *J. Mater. Sci.,* **28,** 4047, (1993).
22. S. Minko, I. Luzinov., I. Evchuk, and S. Voronov, *Polymer,* **37,** 177 (1996).
23. V. S. Kurgansky, V. A. Puchin, S. A. Voronov, and V. S. Tokarev, *Vysokomolekylyarnie Soedinenya Seria A,* **25,** 997 (1983) (Translated to English).
24. L. Lorenzo and T. Hahn, *J. Acoust. Emiss.,* **5,** 15 (1986).
25. J. Wolters, *Fortschr.-Ber. VDI Reihe,* **5**(163) VDI, Düsseldorf, 1989
26. S. Minko, I. Luzinov, and A. Voronov, *Colloid J.,* **56,** 720 (1994)
27. S. Minko, A. Sidorenko, and S. Voronov, *Vysokomolekylyarnie Soedinenya Seria B,* **37,** 1403 (1995) (Translated to English).

Received September 12, 1995
Accepted April 4, 1996